Supplementary information

Tuneable Sulfonated Hypercrosslinked Polymers for Selective Esterification: Insights into Performance and Stability

Paul Schweng,[a,c] Dorian Guerin-Faucheur,[a] Freddy Kleitz,[b]* Robert T. Woodward[a]*

[a] Institute of Materials Chemistry and Research, Faculty of Chemistry, University of Vienna, Währinger Straße 42, 1090, Vienna, Austria

[b] Department of Functional Materials and Catalysis, Faculty of Chemistry, University of Vienna, Währinger Straße 42, 1090 Vienna, Austria

[c] Vienna Doctoral School in Chemistry, University of Vienna, Währinger Straße 42, 1090, Vienna, Austria

Section 1

Experimental

Materials

All chemicals were obtained from commercial sources and used without further purification. Chlorosulfonic acid (99%), 4,4‘-bis(chloromethyl)-1,1‘-biphenyl (95%), 1,2-dichloroethane (≥99%), n-hexadecane (99%), benzyl alcohol (≥99%), hexanoic acid (≥99%), and ethyl acetate (≥99.5%) were purchased from Sigma-Aldrich. Methanol (≥99.8%) and toluene (99.85%, Extra Dry over Molecular Sieve) were purchased from Fisher Scientific.

Synthesis of sulfonated hypercrosslinked polymers

Sulfonated hypercrosslinked polymers (SHCPs) were synthesised with varying catalyst to monomer ratios following a modified literature procedure.[1] 4,4‘-Bis(chloromethyl)-1,1‘-biphenyl (2 mmol, 0.502 g) was first dissolved in 1,2-dichloroethane (DCE, 5 mL) at room temperature. Upon complete dissolution, a solution of chlorosulfonic acid (8, 4, 2, or 1 mmol, corresponding to the formation of SHCP-10, SHCP-7, SHCP-5, and SHCP-3, respectively) in DCE (1 mL) was added, quickly leading to the formation of a brown/black solid. The reaction was heated to 80 °C for 22 h. After cooling, the reaction was quenched with methanol and the resulting brown/black solid was washed with 50 mL of methanol in a Büchner funnel before being washed overnight via Soxhlet extraction, again with methanol. To remove excess methanol, the polymer was initially allowed to dry at room temperature for several hours in the fume cupboard, followed by further drying in a vacuum oven at 80 °C overnight. All samples were produced at least in triplicate to ensure reproducibility.

Esterification reactions using sulfonated hypercrosslinked polymers

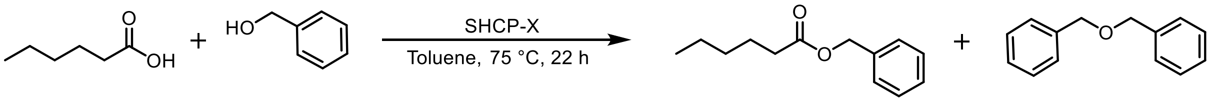

Figure S1. The esterification of hexanoic acid and benzyl alcohol using SHCP as catalyst.

SHCPs were dried at 80 °C overnight in a vacuum oven prior to catalytic experiments as they are hygroscopic.[2] After drying, SHCP (0.05 g) was weighed in a 25 mL round bottom flask fitted with a septum and flushed with dry nitrogen for at least 10 min. The reaction mixture, consisting of benzyl alcohol (5 mmol, 0.517 mL), hexanoic acid (5 mmol, 0.626 mL), and n-hexadecane (0.5 mmol, 0.146 mL, internal standard) in dry toluene (10 mL) was added via syringe under nitrogen flow. The reaction was then initiated by heating to 75 °C. Samples of the supernatant were taken with a syringe at regular intervals under nitrogen flow to monitor reaction progress. The samples were diluted in ethyl acetate before analysis using GC-MS. It is worth noting that all catalysis reactions were repeated at least three times.

Recovery and recycling experiments of sulfonated hypercrosslinked polymers

After the first esterification reaction, SHCP-7 was separated from the reaction mixture via centrifugation. The polymer was washed via redispersion in HCl (1 M) before again being separated by centrifugation. Following a drying step at 80 °C overnight in a vacuum oven, SHCP-7 was redeployed in the succeeding esterification reaction, which was performed under the same conditions.

Characterisation

Fourier-transform infrared spectroscopy (FTIR) measurements were carried out at room temperature using a Tensor II FTIR spectrometer (Bruker) equipped with a Bruker Optics

Platinum ATR module. The IR spectra were measured in the range of 400 - 4000 cm^{-1} with a spectral resolution of 4 cm^{-1} using a double-sided forward–backward acquisition mode. Each spectrum was averaged over a total of 32 scans using a Blackman-Harris 3-term apodisation function with a zero-filling factor of 4. During each measurement, the instrument was purged with dry air and spectra were recorded and analysed using OPUS 7.5 software.

Nitrogen sorption isotherms were recorded at -196 °C on a TriStar II (Micromeritics). The instrument was controlled using TriStar II 3020 software version 3.02. Samples were prepared in a FlowPrep 060 (Micromeritics) at 120 °C under N_2 flow overnight prior to measurement. The acquired data were evaluated using VersaWinTM software version 1.0. The specific surface areas were calculated using the Brunauer-Emmett-Teller (BET) method on the adsorption branch between 0.05-0.20 P/P_0. The volume of N_2 adsorbed at $P/P_0 = 0.97$ was used to calculate the total pore volume, V_{TOT}. The micropore volume, V_{MICRO}, was determined by the t-plot method between 0.15-0.40 P/P_0.

X-ray photoelectron spectroscopy (XPS) was performed on a Nexsa photoelectron spectrometer (Thermo Scientific). High-resolution spectra with a resolution of 0.1 eV and a pass energy of 50 eV were recorded for chlorine (Cl 2p 190-210 eV), sulfur (S 2p 157-175 eV), carbon (C 1s 279-298 eV), nitrogen (N 1s 392-410 eV), and oxygen (O 1s 525-545 eV). All measurements were performed using Al-Kα X-rays with a spot size of 400 μm. Data were analysed using Avantage software (v5.9931, Thermo Fisher Scientific). The main component in C 1s at 284.8 eV was used to calibrate the spectra and the Shirley background was used for peak fitting. The atomic composition of the sample was determined from the peak area using the integrated scaling factor database ALTHERMO1.

Thermogravimetric analyses were carried out on a Discovery TGA (TA instrumentation). Approximately 20 mg of each sample was heated at a rate of 10 °C·min^{-1} from room temperature to 800 °C under N_2 gas flow (100 mL·min^{-1}) and monitored gravimetrically.

The selectivity and conversion of hexanoic acid and benzyl alcohol to the respective ester and ether products was determined using a coupled gas chromatography (Agilent Technologies

7820A with column Agilent 19091S-433) – mass spectrometry (Agilent Technologies 5977B) setup with attached injector (Agilent G4513A). For each measurement, a sample volume of 1 μL was injected and He was used as a carrier gas. The temperature program was as follows: Equilibrate at 60 °C for 1 min, ramp at 15 $°C \cdot min^{-1}$ until 290 °C, isotherm for 3 min. The integrated peak areas were determined using the integrated software (Agilent MassHunter 10.0) and used to calculate conversion and selectivity.

Section 2

Characterisation of sulfonated hypercrosslinked polymers

Fourier-transform infrared spectroscopy

We confirmed the successful formation of sulfonated hypercrosslinked polymers using Fourier-transform infrared spectroscopy (**Figure S2**). The absorption bands at 1473 and 1618 cm^{-1} correspond to C-C stretching vibrations of aromatic carbon in the backbone of all SHCPs. Signals at 1341 cm^{-1} and 1145 cm^{-1} are assigned to asymmetric and symmetric S=O stretching vibrations, respectively. The successful incorporation of sulfonate moieties is further confirmed by a band at 901 cm^{-1} corresponding to S−OH and a characteristic signal for C−S stretching vibrations at 609 cm^{-1}.

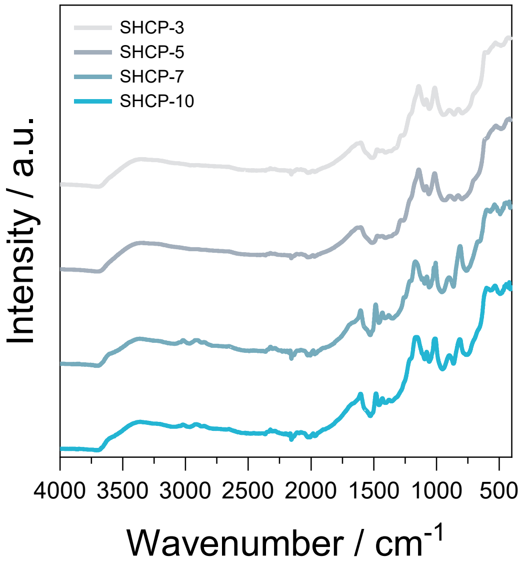

Figure S2. FTIR spectra of SHCP-3, SHCP-5, SHCP-7, and SHCP-10

X-ray photoelectron spectroscopy

We carried out XPS analysis to gain a detailed understanding of the chemical composition of various SHCPs. The high-resolution C 1s spectrum (**Figure S3a**) reveals various functionalities. The major component at a binding energy of 284.8 eV is attributed to C-C bonding, comprising both sp3 and sp2 carbon. A lower intensity peak observed at 286.8 eV corresponds to C-S. A broad, low intensity π-π* shake-up feature is also observed at 290.8 eV. The incorporation of sulfonic acid moieties was confirmed by the characteristic asymmetric shape observed in the high-resolution S 2p spectrum (**Figure 3b**), and peaks at binding energies of 168.7 eV and 169.8 eV are attributed to S $2p_{3/2}$ and S $2p_{1/2}$, respectively.

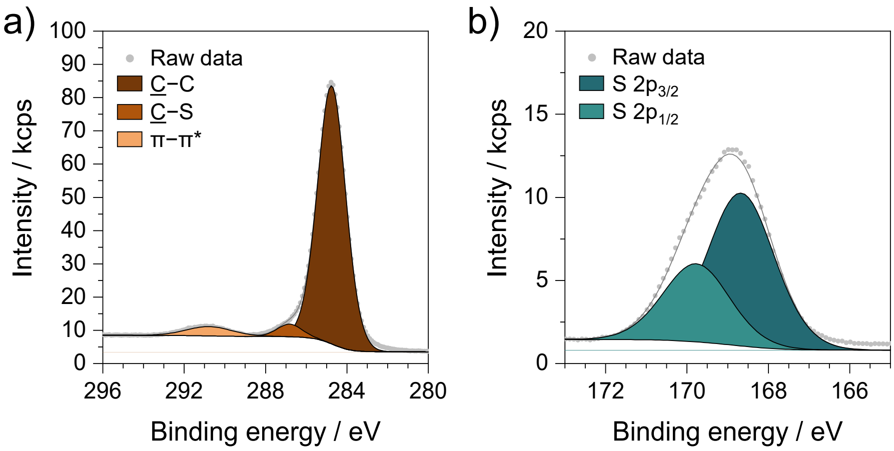

Figure S3. High-resolution X-ray photoelectron a) C 1s and b) S 2p spectra for SHCP-7

The surface chemical compositions determined by XPS are given in **Table S1**. Increasing the catalyst to monomer ratio led to higher sulfonation densities, in good agreement with our previous report.[1]

Table S1. Elemental composition of SHCP-10, SHCP-7, SHCP-5, and SHCP-3 derived from XPS analysis. Data are provided as mean ± standard deviation (n = 3).

	Catalyst:monomer	C (wt.%)	N (wt.%)	O (wt.%)	Cl (wt.%)	S (wt.%)
SHCP-10	4	63.5 ± 2.2	0.7 ± 0.1	19.6 ± 2.0	1.9 ± 0.4	14.2 ± 0.8
SHCP-7	2	68.1 ± 1.0	0.4 ± 0.1	18.7 ± 0.2	1.9 ± 0.1	10.9 ± 1.3
SHCP-5	1	78.8 ± 2.4	0.3 ± 0.2	11.3 ± 1.6	2.7 ± 0.7	7.0 ± 1.0
SHCP-3	0.5	83.1 ± 2.6	0.5 ± 0.3	9.3 ± 2.0	3.0 ± 0.4	4.1 ± 0.5

Nitrogen gas sorption analysis

We collected N_2 sorption isotherms to gain information on the textural properties of SHCPs (**Figure S4**). The presence of microporosity is evidenced by a steep uptake at low relative pressures and mesoporosity/macroporosity was confirmed by the emergence of hysteresis during desorption. All samples exhibited characteristics of both type I and type IVa isotherms and H2 hysteresis curves, indicating broad pore size distributions with narrow pore necks.

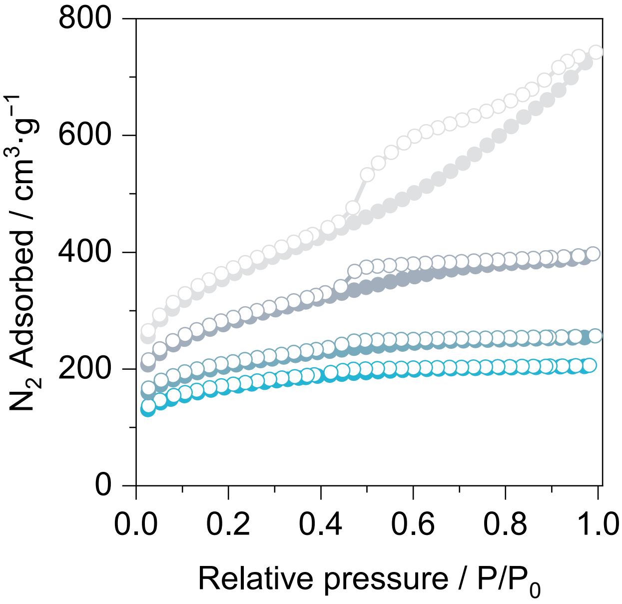

Figure S4. N_2 sorption-desorption isotherms of SHCP-3, SHCP-5, SHCP-7, and SHCP-10 measured at −196 °C.

Thermogravimetric analysis

We analysed the thermal stability of all SHCPs using thermogravimetric analysis (TGA) in an inert N_2 atmosphere (**Figure S5**). The initial weight loss below 100 °C is attributed to water desorption in all samples and increases dramatically with sulfonation density. All samples were stable up to a temperature of ~200 °C, confirming good thermal stability.

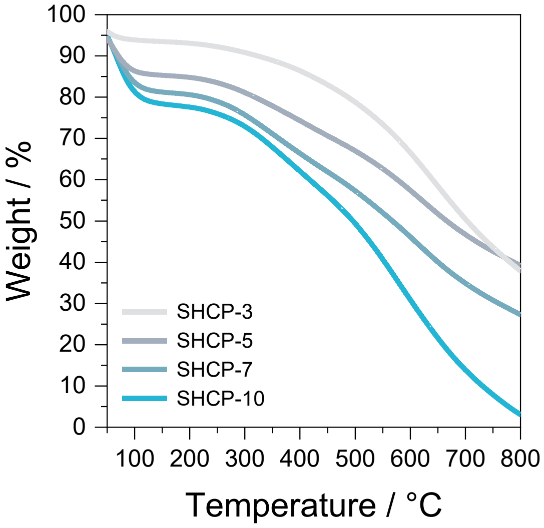

Figure S5. Thermogravimetric curves for SHCP-3, SHCP-5, SHCP-7, and SHCP-10 heated up to 800 °C at a ramp rate of 10 $°C{\cdot}min^{-1}$ under N_2 flow.

Section 3

Catalysis experiments

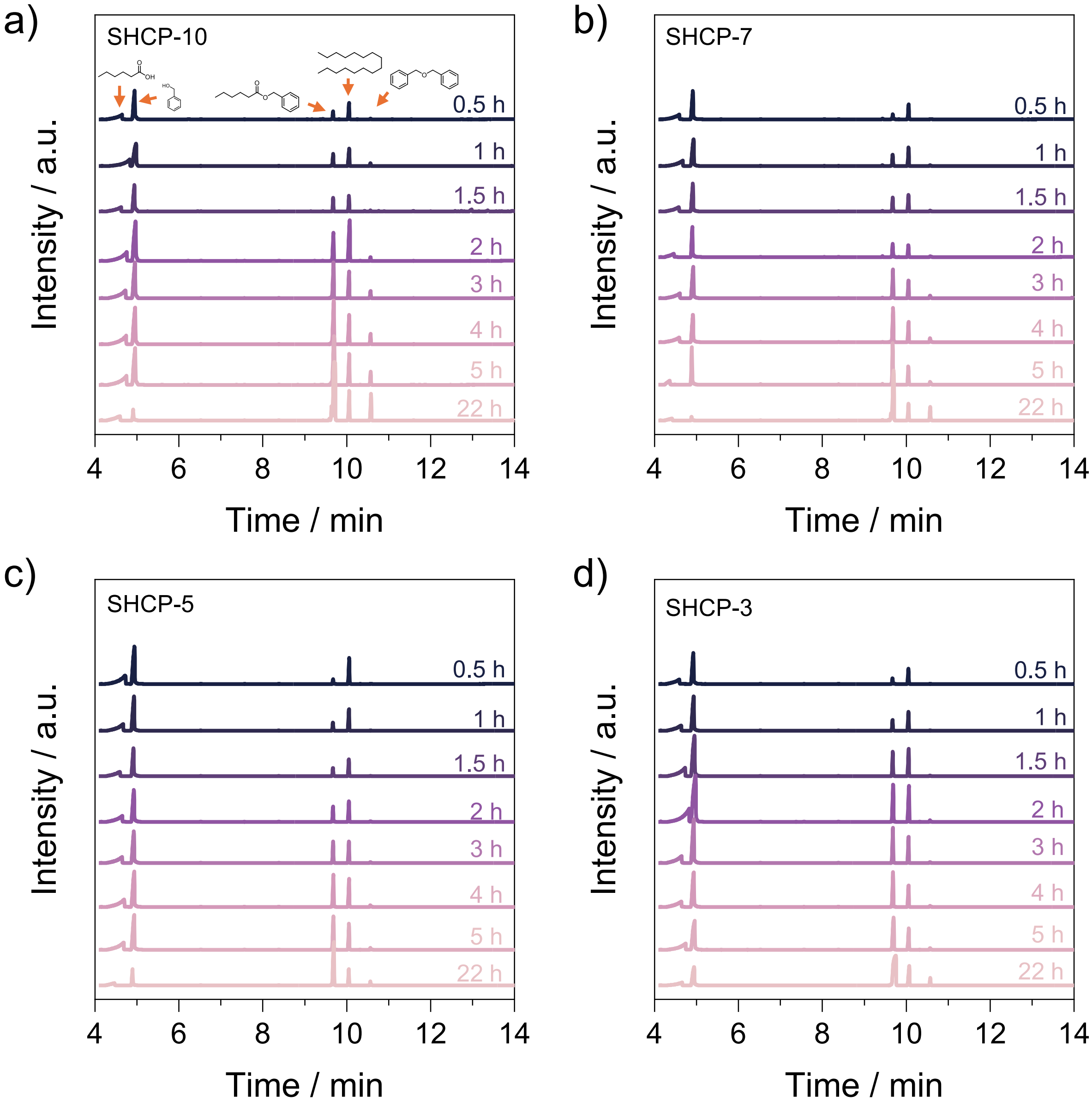

Figure S6. Representative chromatograms for each SHCP as the reaction progressed over time.

Table S2. Benzyl alcohol conversion over time for each SHCP and a non-sulfonated HCP control. Data are provided as mean ± standard deviation (n = 3).

Time / h	Benzyl alcohol conversion / %				
	Non-sulfonated	SHCP-3	SHCP-5	SHCP-7	SHCP-10
0.5	0	7 ± 4	7 ± 2	11 ± 1	11 ± 3
1	0	9 ± 5	13 ± 3	17 ± 2	21 ± 1
1.5	0	13 ± 7	17 ± 3	26 ± 2	25 ± 4
2	0	16 ± 7	22 ± 4	33 ± 4	31 ± 3
3	0	22 ± 8	31 ± 4	42 ± 5	39 ± 4
4	0	26 ± 10	36 ± 5	52 ± 7	46 ± 5
5	1	30 ± 10	40 ± 7	59 ± 5	52 ± 5
22	6	61 ± 12	82 ± 3	95 ± 4	91 ± 6

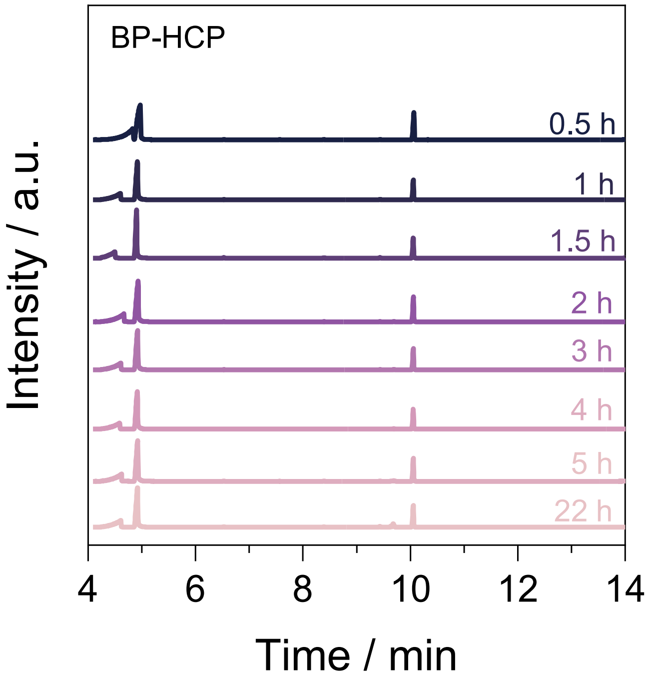

Figure S7. Chromatograms of non-sulfonated HCP control.

Table S3. Ester/ether selectivity over time for each SHCP and a non-sulfonated HCP control. Data are provided as mean ± standard deviation (n = 3).

Time / h	Ester/ether selectivity / mol·mol^{-1}				
	Non-sulfonated	SHCP-3	SHCP-5	SHCP-7	SHCP-10
0.5	-	24 ± 3	21 ± 1	7 ± 3	5 ± 1
1	-	28 ± 4	23 ± 1	8 ± 3	6 ± 1
1.5	-	28 ± 2	24 ± 3	8 ± 3	6 ± 1
2	-	27 ± 2	23 ± 3	9 ± 3	8 ± 2
3	-	30 ± 4	24 ± 4	8 ± 2	8 ± 2
4	-	29 ± 3	22 ± 3	8 ± 2	8 ± 2
5	-	27 ± 2	21 ± 3	8 ± 2	8 ± 2
22	-	19 ± 5	15 ± 3	6 ± 1	7 ± 1

Table S4. Comparison of benzyl alcohol conversion and ester/ether selectivity for a variety of catalysts reported in the literature.

Material	Benzyl alcohol conversion / %	Ester/ether selectivity / mol·mol^{-1}	Reference
Sulfuric acid	92	30	3
Composite 30%	98	6	3
NMP2-DVB-100	93	8	3
NMP2-PS-30	98	17	3
Nafion NR50	96	6	4
Resin 1	96	105	4
Amberlyst-15	38	6	5
10-SPS-C	98	51	5
20-SPS-C	97	27	5
30-SPS-C	97	11	5
SHCP-3	61	19	This work
SHCP-5	82	15	This work
SHCP-7	95	6	This work
SHCP-10	91	7	This work

Section 4

Recycling experiments

Table S5. Benzyl alcohol conversion and ester/ether selectivity for SHCP-7 cycling experiments. Conversion and selectivity were determined after 22 h of reaction.

Cycle	Benzyl alcohol conversion / %	Ester/ether selectivity / mol·mol^{-1}
1	95 ± 4	8 ± 2
2	87	5
3	65	3
4	53	3
5	27	3

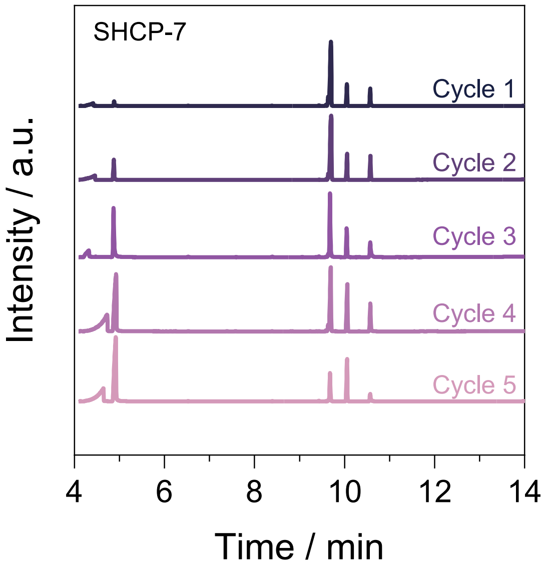

Figure S8. Chromatograms from SHCP-7 cycling experiments. Each chromatogram was recorded after 22 h of reaction.

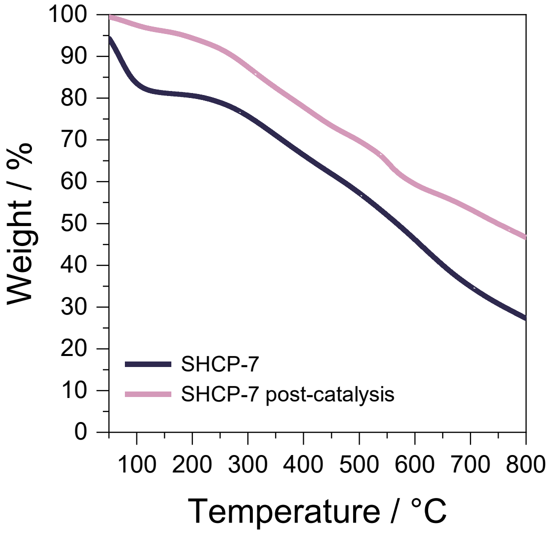

Figure S9 Thermogravimetric curves for heated up to 800 °C at a ramp rate of 10 °C·min^{-1} under N_2 flow of SHCP-7 before (navy blue) and after (pink) 5 catalytic cycles.

Table S6. Elemental composition of SHCP-7 before and after 5 catalytic cycles derived from XPS analysis.

	C (wt.%)	N (wt.%)	O (wt.%)	Cl (wt.%)	S (wt.%)
SHCP-7	68.1 ± 1.0	0.4 ± 0.1	18.7 ± 0.2	1.9 ± 0.1	10.9 ± 1.3
SHCP-7 post-catalysis	70.2	0.7	20.2	0.4	8.6

References

---

[1] A. Blocher, F. Mayer, P. Schweng, T. M. Tikovits, N. Yousefi and R. T. Woodward, *Mater. Adv.*, 2022, **3**, 6335–6342.

[2] P. Schweng, F. Mayer, D. Galehdari, K. Weiland and R. T. Woodward, *Small*, 2023, **19**, 2304562.

[3] S. Bilodeau, J. Florek and F. Kleitz, *Chem. Ing. Tech.*, 2021, **93**, 916–928.

[4] Y. Xu, W. Gu, D. L. Gin, *J. Am. Chem. Soc.*, 2004, **126**, 1616–1617.

[5] M. Choi, F. Kleitz, D. Liu, H. Y. Lee, W.-S. Ahn and R. Ryoo, *J. Am. Chem. Soc.*, 2005, **127**, 1924–1932.